PHYSICAL REVIEW B VOLUME 21, NUMBER 2 15 JANUARY 1980

Hartree band structure, Fermi surface, and nesting wave vector for paramagnetic chromium

J. L. Fry, N. E. Brener, J. L. Thompson, and P. H. Dickinson
University of Texas at Arlington, Arlington, Texas 76019
(Received 9 February 1979)

In this paper it is demonstrated that it is possible to predict the wave vector of the spin-density wave in chromium without explicit consideration of exchange and correlation effects. To do so the Fermi surface is obtained from a Hartree energy-band calculation and used to deduce the nesting wave vector. In this process the Fermi surface is presented using computer-graphic techniques which give clear views of the Fermi surface and its nesting portions. The Fermi surface and nesting wave vector are found to change dramatically as self-consistency is achieved in the energy-band calculation. For the self-consistent potential, agreement with the experimentally determined nesting wave vector is found to within about ten percent. It is concluded that the dominant exchange and correlation effects needed to establish the spin-density wave are implicitly included when the experimental lattice constant, lattice structure, and number of electrons per atom are introduced into the energy-band calculation.

I. INTRODUCTION

The energy-band structure and Fermi surface of chromium have been of continued interest since it was first suggested that the ground state of chromium contains a spin-density wave.[1,2] Numerous band calculations exist for paramagnetic chromium, most of which included some approximation to exchange effects but none to correlation effects, and most of which were performed without consideration of self-consistency between the charge distribution and the crystal potentials employed.[3-10] The most thorough calculation was performed by Rath and Callaway, who gave a brief review of the earlier ones, including the various exchange and correlation methods used and the amount of self-consistency achieved.[10] That discussion is adequate and will not be repeated here.

Most of the studies cited above attempted to obtain the wave vector of the spin-density wave by examining the Fermi surface for nesting features, as suggested by Lomer.[1] A more rigorous approach was used by Gupta and Sinha,[9] who obtained the nesting wave vector by calculation of the wave-vector dependence of the magnetic susceptibility $\chi(\vec{q})$. An absolute maximum of $\chi(\vec{q})$ for $\vec{q}_0 \neq 0$ is the condition used to predict stability of a spin-density wave at wave vector $\vec{q}_0$.[11] More elaborate conditions for the temperature dependence of a paramagnetic to antiferromagnetic transition have been discussed by Fedders and Martin,[12] and Asano and Yamashita.[7] Conditions for antiferromagnetism have also been given by Yamashita *et al.*[13]

A number of developments in recent years have motivated a reexamination of the spin-density wave in chromium. First, band-structure methods have improved considerably so that accurate, self-consistent results may now be obtained by a variety of methods. New treatments of exchange and correlation within the framework of energy-band theory have been developed, and new formulas for the susceptibility of an electron system including exchange and correlation have evolved. These developments are discussed in various review articles and in the text by Callaway.[14,15] Equally important has been the development of fast numerical procedures for evaluating $\chi(\vec{q})$.[16]

Before embarking on a more lengthy computational effort which would reexamine the significant work of Gupta and Sinha[9] in light of these new developments, it was determined that a simpler study was first appropriate. In a recent article[17] two authors of this paper used the Green's-function method of Hedin[18] to go beyond the random-phase approximation (RPA) to the susceptibility to include exchange and correlation in a systematic fashion, and noted that the usual RPA formula should employ Hartree energies and matrix elements to be consistent with the theory from which it is derived. For the electron gas it was shown that substantially different results are obtained when different choices for input energies are made in calculating $\chi(\vec{q})$. This further motivated the present study for a real metal using Hartree solutions for electrons moving in the periodic chromium lattice.

This paper reports the Hartree energy-band structure of paramagnetic chromium and analyzes it for the density of states, Fermi surface, and nesting wave vector. The importance of self-consistency is stressed by comparing results from a typical potential constructed as a superposition of atomic potentials with those achieved after self-consistency was established for the crystal potential. The resulting nesting wave vector is estimated from the corresponding Fermi surfaces, and surprisingly good agreement

is achieved between the experimentally determined wave vector of the spin-density wave and the self-consistent Hartree value, in spite of the failure to include explicitly exchange and correlation contributions either in the band structure or the susceptibility function.

The remainer of this paper is outlined as follows. Section II briefly presents the energy-band calculations and the densities of states. In Sec. III the Fermi surfaces for the starting potential and the self-consistent potential are analyzed by contour plots and by some interesting computer-graphic studies. Section IV discusses the nesting-wave-vector determinations and Sec. V states the conclusions which are drawn from this study.

II. ENERGY BANDS

The energy-band structure of paramagnetic chromium was determined from a Hartree calculation using a body-centered-cubic (bcc) lattice constant $a = 5.45$ a.u. The linear combination of atomic orbitals (LCAO) method employed here has been described elsewhere,[19-21] and is similar to the method used by Rath and Callaway in a Hartree-Fock-Slater calculation for paramagnetic chromium.[10] The LCAO basis set was adapted for solid chromium from the basis set used by Wachters in an atomic calculation.[22] Contraction coefficients were used to save computer time and core and a 41×41 Hamiltonian matrix resulted. In order to obtain well-converged energy bands, special attention was paid to convergence of lattice sums as well as convergence with respect to the basis set. Energy eigenvalues are believed converged to within 0.001 Ry for the bands of interest here. No effort was made to include f-symmetry orbitals or spin-orbit interactions. In this Hartree calculation exchange and correlation terms in the Hamiltonian were purposely omitted.

The band structure for the starting crystal potential is shown in Fig. 1. The potential was constructed as a superposition of atomic potentials (AS) corresponding to a $3d^5 4s^1$ configuration.

The final self-consistent (SC) potential was obtained by allowing changes in the first thirty independent Fourier coefficients of the potential until all coefficients were converged to within 0.0001 Ry. A 55-point grid in 1/48 of the bcc Brillouin zone was used to generate the iterated Fourier coefficients of the potential. The first and last iterations were done with 819 points to provide accurate Fermi surfaces. By carefully determining the Fermi energy at each iteration, no convergence problems were encountered. The fully self-consistent Hartree energy bands are shown in Fig. 2, after 11 iterations.

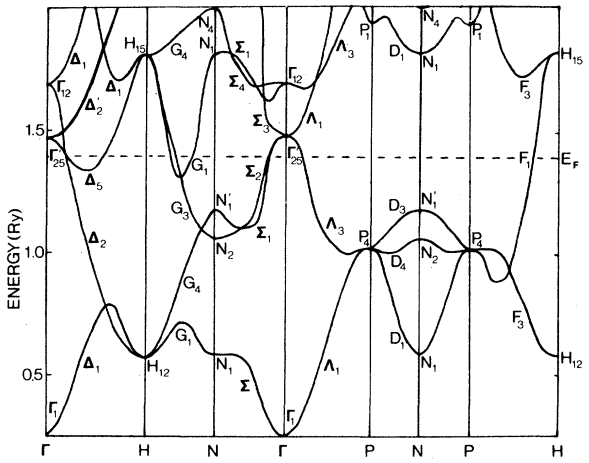

FIG. 1. Hartree energy bands of paramagnetic chromium along symmetry directions for the superposition of atomic potentials.

A comparison of Figs. 1 and 2 reveals that important changes occurred between the first and last iterations. The most significant change was the position of levels at H. Because of inconsistency between the basis and the atomic superposition (AS) potential, the p-like level H_{15} fell below the d-like level H'_{25}. This order reversed as self-consistency lowered and narrowed the d bands. This is visible in the densities of states for the two band strcutres in Fig. 3 (AS) and Fig. 4 (SC). These densities of states were obtained using the analytic tetrahedron method[16] with a grid of 3456 tetrahedra in 1/48 of the first Brillouin zone and an energy interval of 0.005 Ry. The scale sizes are different to show details in Figs. 3 and 4. The Fermi energies (E_F) obtained by integrating the density of states were 1.393 and 0.939 Ry, respectively, or 1.142 and 9.714 Ry, respectively, relative to the bottom of the con-

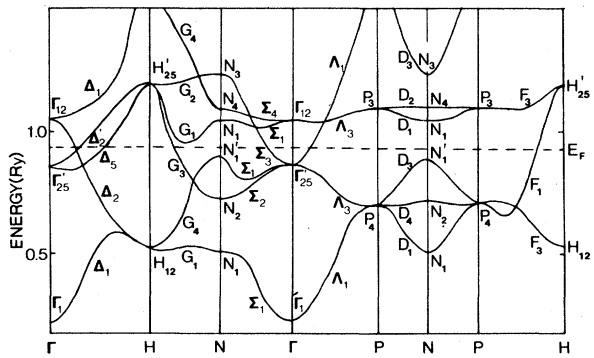

FIG. 2. Hartree energy bands of paramagnetic chromium along symmetry directions for the self-consistent potential.

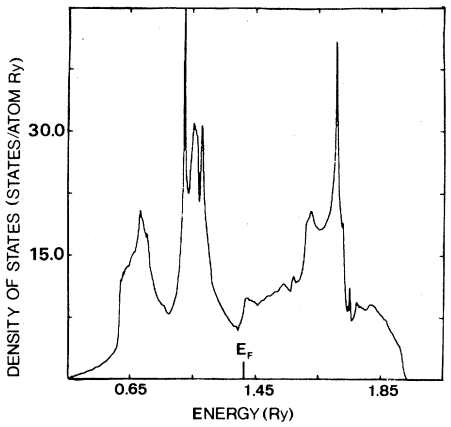

FIG. 3. Hartree density of states for chromium for the atomic superposition potential. The analytic tetrahedron method was used with 3456 equal-volume tetrahadra in $\frac{1}{48}$ of the Brillouin zone and an energy interval of 0.005 Ry.

duction bands Γ_1. The latter self-consistent Fermi energy may be compared with a Hartree-Fock-Slater value of 0.53 Ry deduced from Fig. 2 of Ref. 10, or 0.64 Ry from Ref. 9. These differences are traced to self-consistency effects and the fact that Gupta and Sinha,[9] and Rath and Callaway[10] included exchange potentials which caused a lowering and narrowing of the conduction bands. The band structure of Gupta and Sinha was not self-consistent, so additional lowering of their energy is expected with a corresponding reduction of E_F relative to Γ_1.

It is not the purpose of this paper to make detailed comparisons with other energy-band calculations for chromium, since this is only a Hartree calculation. For such comparison some of the energy levels at symmetry points are given in Table I. The point to be stressed here is that

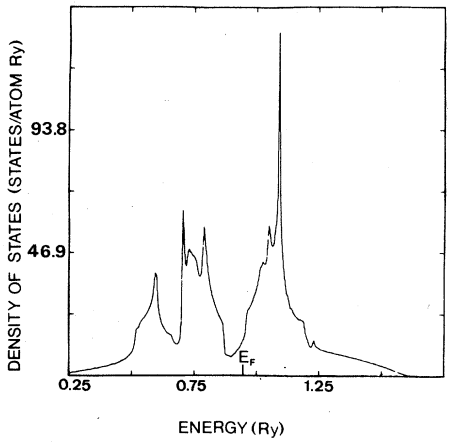

FIG. 4. Hartree density of states for chromium for the self-consistent potential.

TABLE I. Self-consistent energy bands of paramagnetic chromium at symmetry points. Energy in rydbergs.

Γ_1	Γ'_{25}	Γ_{12}	H_{12}	H'_{25}	H_{15}
0.2247	0.8742	1.0457	0.5288	1.1908	1.5970
N_1	N_2	N'_1	N_1	N_4	N_3
0.5162	0.7251	0.8991	1.0524	1.0867	1.2294
P_4	P_3	P_4	E_F		
0.7111	1.0924	1.6876	0.939		

self-consistency has dramatic effects upon the band structure in this LCAO study, as can be seen by comparing Figs. 1 and 2 or Figs. 3 and 4. The self-consistent band structure is similar to the Hartree-Fock-Slater results of Rath and Callaway,[10] the chief difference being the order of levels at the point N. Inclusion of their exchange potential into the energy-band calculation of this paper should yield essentially identical results, since the methods are identical, and both calculations are converged. It is surprising that even better agreement is obtained in the band structure of Gupta and Sinha,[9] although their band structure is not self-consistent and the present results exclude exchange. Exchange entered this computation only indirectly: Hartree-Fock wave functions were used to generate the starting charge density from which the Coulomb potential of the electrons was obtained. In view of the large changes which occurred here, it is necessary to express strong reservations about the details of the band structure of Gupta and Sinha in comparison with that of Rath and Callaway, which was self-consistent. How these differences might affect the susceptibility function $\chi(q)$ is not obvious, but matrix elements and positions of peaks in $\chi(q)$ are surely affected.

A comparison of the SC Hartree density of states, Fig. 4, with the SC Hartree-Fock density of states of Ref. 10 shows qualitative agreement on all structures that are readily observable in the figures. Although the level N'_1 lies below the Fermi energy in the former and above in the latter, there is no corresponding structure in the density of states which is detectable. Aside from different band widths, the main observable difference is caused by reversal of the levels P_4 and N_2 between the two calculations, which causes the broad peak in Fig. 4 at 0.75 Ry which is not present in Ref. 10. This small difference is reflected in the Fermi surface, as described below.

On the other hand, the SC Hartree and AS Hartree densities of states are noticeably different. The most important change upon achieving self-

consistency is the increase in strength of the peak above the density of states which arises from the bands in the vicinity of D_2, N_4, P_3, and F_3 (at about 1.1 Ry in the SC density of states). The Fermi surfaces for the two Hartree band structures differ more dramatically.

III. FERMI SURFACES

Fermi energies for the AS and SC Hartree band structures were determined by integration of the densities of states. The Fermi surfaces were first investigated by contour plots in planes perpendicular to the k_z axis. The plane $k_z = 0$ for the two calculations is shown in Fig. 5 (AS) and Fig. 6 (SC).

The Fermi-surface sections shown in Fig. 5 consist of surfaces in three conduction bands. For analysis of the energy-band structure producing these surfaces, it is convenient to define band one as the set of levels which lies lowest in energy at each point in k space, band two as the set of energies which lies next lowest, etc. With this notation the symmetry type of a band will change at each band intersection, but the Fermi-surface topology is more easily understood. For convenience the Γ_1 conduction level is defined to be the bottom of the first band, additional lower bands being ignored. With the definition for a band introduced above, this band (number one) is completely filled, and thus does not contribute to conduction at all. The second, third, and fourth bands intersect the Fermi energy. Band two ($\Delta_5 - \Delta_2 - \Delta_1$, etc. in Fig. 1) has a hole surface at Γ (vertical markings); band three has two hole surfaces, one at Γ (enclosing the hole surface of band two) and the other at H; band four has an electron surface surrounding, but not including, H. It is possible but difficult to visualize these Fermi surfaces in three dimensions by using a succession of contour plots, so computer-graphic-imaging methods were employed.[23]

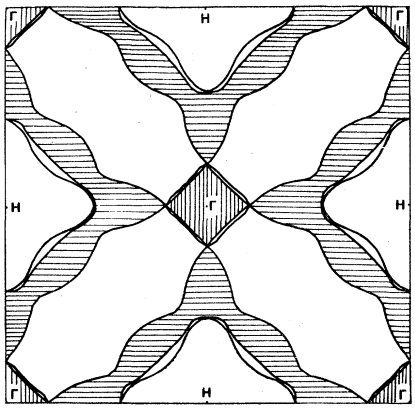

FIG. 5. Cross sections of the Fermi surface in the plane $k_z = 0$ for the atomic superposition potential. Band-two surface is centered at Γ and indicated with vertical lines. Band three has two sections, one at Γ and one at H. Band four is indicated with horizontal lines. Figure 7 shows bands three and four in perspective.

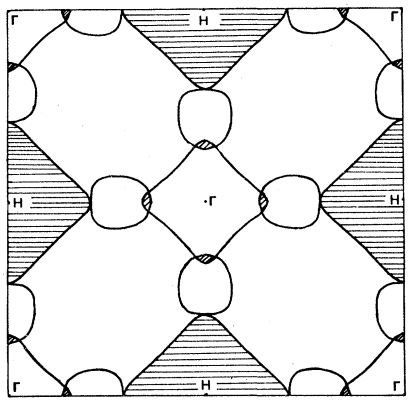

FIG. 6. Cross sections of the Fermi surface of chromium in the plane $k_z = 0$ from the self-consistent potential. Band three is a hole surface around H; band four is the electron jack; and band five is a set of electron lenses contained in the neck of the jack (diagonal lines).

The computer-graphic method allowed viewing of the different Fermi-surface pieces from various angles. This was especially useful for the AS Fermi surface which is complex and had not been examined previously. The band structures were generated at 819 points in 1/48 of the first Brillouin zone and interpolated to give a total of over 4000 points. The graphics package was used to obtain three-dimensional projective drawings by straight-line connection of these points, including proper scaling and hiding of lines to give perspective. Shading in with colored felt tip pens enhances depth perception of these images.

For the AS Fermi surface, bands three and four are shown from the same perspective in Figs. 7(a) and 7(b). The band-two surface is similar to the central part of the band-three surface and is not shown. The electron surface at H in Fig. 7(b) forms a complicated but interesting figure when the origin is chosen at H, consisting of six of the claw-like figures connected around the point H. These Fermi surfaces [Figs. 7(a) and 7(b)] are unlike any others published for paramagnetic chromium (or any other metal) and must be an artifact of the AS potential or basis set used here, neglect of exchange, or lack of self-consistency. The latter seems to be the most important, as discussed below.

The self-consistent Fermi-surface contours in

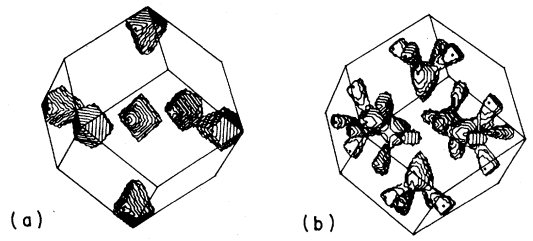

FIG. 7. (a) Band-three hole surfaces of chromium from the atomic superposition potential. Cross sections in the plane $k_z = 0$ areshown in Fig. 5. (b) Band-four electron surfaces of chromium from the atomic superposition potential. Six of these electron "claws" are connected through the surfaces of the zone to form a complex surface surrounding the point H. Cross sections in the plane $k_z = 0$ are shown in Fig. 5.

Fig. 6 are more familiar. With the same band-numbering scheme as before, there are once again three sections of the Fermi surface. Bands one and two lie completely below the Fermi level. Band three has a hole octrahedron centered at H, band four is the familiar electron jack, and band five is a set of electron lenses inside the necks of the jacks (diagonal lines). The first two surfaces are shown in Figs. 8(a) and 8(b). The lenses are too small to plot well on the scale of these figures. Missing in these figures are the hole pockets at N (which look like jelly beans) as reported in Hartree-Fock-Slater band structures. Figures 9 shows a composite of the two Fermi surfaces responsible for the nesting wave vector in chromium. This plot is obtained from a large number of computed points in the Brillouin zone and is viewed from an angle similar to the one used by Mattheiss in his sketch of the Fermi surface of chromium. A view including the entire structure at each point H is remarkably similar to Mattheiss' model, which was drawn without benefit of an energy-band study for chromium.[24] It is impressive how well Lomer and Mattheiss

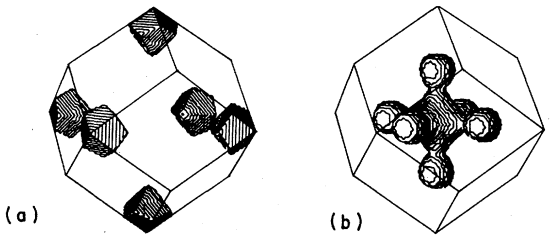

FIG. 8. (a) Band-three hole surfaces for chromium from the self-consistent potential. Cross sections in the plane $k_z = 0$ are shown in Fig. 6. (b) Band-five electron surfaces for chromium from the self-consistent potential. Cross sections in the plane $k_z = 0$ are shown in Fig. 6.

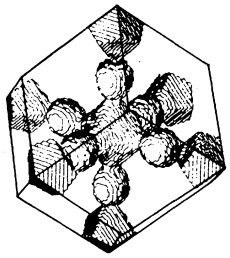

FIG. 9. Nesting portions of the Fermi surface of chromium. The hole surfaces at H are just tangent to the balls of the electron jack along the cubic axis. When one of these surfaces is shifted by $0.90(2\pi/a)$ along a Δ axis, it nests with the body of the electron jack at Γ.

were able to anticipate the band structure of paramagnetic chromium by using information from other transition metals and the rigid-band concept.

The dramatic change which occurred when a self-consistent potential was employed led to much better agreement with experimental information and with previous band calculations. To investigate whether the inclusion of exchange would have the same effect, a non-self-consistent calculation was performed using the X_α local exchange potential approximation with $\alpha = \frac{2}{3}$, the value employed in Ref. 10.

As expected, inclusion of the exchange potential had the effect of lowering the conduction bands and the Fermi level, changing the Fermi surface significantly, as can be seen in Figs. 10, 11(a), and 11(b), Figure 10 corresponds to Fig. 5, and it can be seen that the main effect of including exchange is a spilling over of electrons into the two hole surfaces at Γ, until the electron claws join

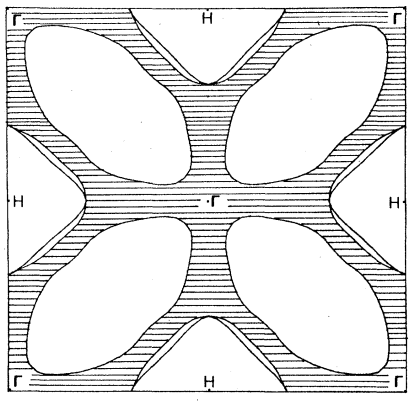

FIG. 10. Cross sections of the Fermi surface of chromium in the plane $k_z = 0$ from the non-self-consistent X_α potential. Band three is a hole surface around H; band four (horizontal lines) is an electron surface; and band five is a set of thin electron lenses contained within the arms of the electron surface of band four.

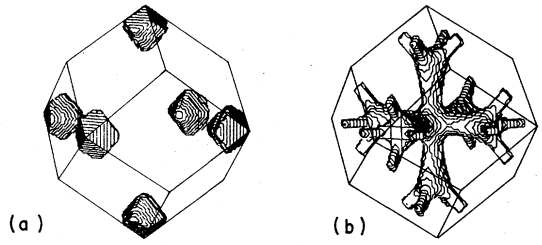

FIG. 11. (a) Band-three hole surfaces for chromium from the X_α potential, not self-consistent. (b) Band-four electron surface for chromium from the X_α potential, not self-consistent. The evolution of the electron jack can be seen in Figs. 7(b), 11(b), and 8(b) as exchange and self-consistency are added to the crystal potential.

up and the holes disappear. A comparison of Figs. 7(a) and 11(a), and Figs. 7(b) and 11(b) reveals the changes clearly. While they are noticeable, they do not produce a good Fermi surface in comparison with Fig. 8. Not shown in Figs. 10 and 11 are a set of electron lenses similar to the ones in Fig. 6, but too small to plot accurately without more extensive Brillouin-zone sampling than was done here. Missing from this X_α calculation is the set of hole pockets around the points N. They appear only after self-consistency is achieved including exchange.

IV. NESTING WAVE VECTOR

A proper determination of the wave vector of the spin-density wave in chromium requires calculation of $\chi(\vec{q})$, which is a nontrivial task, to say the least. Gupta and Sinha accomplished it with an augmented-plane-wave (APW) band structure followed by a major computational effort to evaluate $\chi(\vec{q})$. The band structure was not self-consistent, but did include exchange in an approximate way. Their susceptibility functions exhibited a maximum at $\vec{q} = 2\pi/a$ (0.88, 0, 0), but they did not quote any Fermi-surface dimensions for comparison.[9]

To estimate the nesting wave vector for the Hartree band structures reported here, contour plots and computer-graphic methods have been employed. For the AS Hartree band structure a number of possible nestings occur, but none of them strong enough to produce an absolute maximum in $\chi(q)$. The strongest nesting occurs between the hole surface in band three centered at Γ with the inside of electron claws along the Δ axis. This is best visualized by making transparency overlays for Figs. 5 and 7 and other computer-graphic views. From Fig. 5 the nesting vector is about (0.74–0.78) $2\pi/a$. This range of nesting vectors for the AS Fermi surface is similar to that found in Ref. 10, but it should be observed that the electron and hole surfaces are quite different here, and in fact, interchanged positions. A preliminary calculation of $\chi(\vec{q})$ along the Δ axis using the analytic-tetrahedron method[16] with constant matrix elements produced only a very weak relative maximum in the vicinity of $q = 0.8(2\pi/a)$.[25]

The X_α potential produced a Fermi surface with a nesting vector which corresponds to the body of the electron surface at Γ nesting with the hole octahedron at H. The nesting is not strong in the sense of occurring over a large area, but it is similar to the SC-potential nesting behavior for the Fermi surface. Once again a nesting vector occurs at 0.8 $(2\pi/a)$, but another nesting occurs which appears stronger at about 0.05 $(2\pi/a)$. The latter corresponds to a nesting of the hole octahedron at H with the palm of the claw extending along Δ toward H. The claws vanish with self-consistency to form balls on the electron jack discussed below.

The SC Hartree band structure exhibits much stronger nesting features which suggest that conditions could be right for the spin-density wave. From Figs. 6, 8, and 10 the dominant nesting feature is the one between the body of the electron jack at Γ and the hole octahedron at H. The nesting vector along the Δ axis ranges from 0.88 to 0.90 $(2\pi/a)$ over a large area of the Fermi surface. This is made more apparent by the use of transparencies of the computer-graphic images viewed from different perspectives. In order to accurately determine the nesting vector, a full calculation of $\chi(\vec{q})$ including matrix elements and local-field effects must be performed. However, this approximate determination of q_0 using Hartree-Fermi surfaces gives values close to those obtained by Gupta and Sinha[9] and also the experimental values of Koehler *et al.*[26] Near the phase transition temperature experiment yields $q_0 = 0.963\ (2\pi/a)$. The Hartree value of q_0 is essentially the same as that obtained from the elaborate calculation of Gupta and Sinha, and is in error compared to the experimental values by less than ten percent. A complete calculation of $\chi(q)$ is required to verify the Hartree value of q_0 since matrix-element and local-field effects are thought to be significant, but it seems likely the Hartree value will lie in the range obtained by Fermi-surface nesting measurements. It would be interesting to compare the predictions for q_0 from an RPA susceptibility calculation using these Hartree energy bands and wave functions with the predictions from the time-dependent Hartree-Fock susceptibility function using Hartree-Fock energy bands and wave functions.

V. CONCLUSION

A well-converged LCAO Hartree energy-band calculation for a starting crystal potential for paramagnetic chromium gave a band structure with an unusual Fermi surface and an order of energy levels contrary to previous experience. This was caused mostly by lack of self-consistency, and only partly by lack of exchange. Even without the exchange potential, the self-consistent Hartree bands resemble very closely the band structures which have been obtained by others using exchange and different starting potentials. Inclusion of exchange in this study improved the non-self-consistent band structure only slightly. While the self-consistent Hartree band structure obtained here agrees fairly well with the Hartree-Fock-Slater band structure of Gupta and Sinha, their results are likely to change when made self-consistent, unless they made a much better approximation for the starting potential than was made here. The self-consistent Hartree-Fermi surface lends further support to the Fermi-surface model originally proposed by Lomer.

The nesting wave vector determined from the well-converged, self-consistent Hartree structure by Fermi-surface determinations is in agreement with the susceptibility results of Gupta and Sinha, but differs slightly from the Fermi-surface dimensions of Rath and Callaway. This is the interesting conclusion to be made by this paper: It is possible to obtain an accurate estimate of the wave vector of the spin-density wave of chromium without explicit consideration of exchange effects. The nesting wave vectors appears to be mostly a topological effect produced when the proper lattice constant, lattice structure, and number of electrons per atom are once established. These quantities themselves all depend upon a minimum in the total energy of the crystal, and consequently include exchange and correlation effects implicitly. One might then infer that the pressure dependence of the paramagnetic-antiferromagnetic phase transition in chromium could be deduced by repeating the Hartree calculation at appropriate lattice constants to find a critical pressure at which the nesting features of the Fermi surface are lost. Such a study will be reported in a future paper.

ACKNOWLEDGMENTS

This research was supported by the U.S. AFOSR under Grant No. AFOSR-76-2981. During part of this research J. L. Thompson received the support of the Robert A. Welch Foundation. P. H. Dickinson acknowledges support of the N.S.F.-Student Science Training Program. The assistance of Mr. Duane Laurent is gratefully acknowledged in using the band-package[27] program BNDPKG to produce the non-self-consistent X_α band structure of paramagnetic chromium.

[1]W. M. Lomer, Proc. Phys. Soc. London 80, 489 (1962).
[2]W. M. Lomer, Proc. Phys. Soc. London 84, 327 (1964).
[3]M. Asdente and J. Freidel, Phys. Rev. 124, 384 (1961).
[4]M. Asdente, Phys. Rev. 127, 1949 (1962).
[5]T. L. Loucks, Phys. Rev. 139, A1181 (1965).
[6]A. C. Switendick, J. Appl. Phys. 37, 1922 (1966).
[7]A. Asano and J. Yamashita, J. Phys. Soc. Jpn 23, 714 (1967).
[8]M. Yasui, E. Hayashi, and M. Shimizu, J. Phys. Soc. Jpn 29, 1446 (1970).
[9]R. P. Gupta and S. K. Sinha, Phys. Rev. B 3, 2401 (1971).
[10]J. Rath and J. Callaway, Phys. Rev. B 8, 5398 (1973).
[11]C. Herring, in *Magnetism*, edited by G. Rado and H. Suhl (Academic, New York, 1966), Vol. 4; see also Ref. 14 below.
[12]P. A. Fedders and P. C. Martin, Phys. Rev. 143, 245 (1966).
[13]J. Yamashita, S. Asano, and S. Wakoh, J. Appl. Phys. 39, 1274 (1968).
[14]J. Callaway, *Quantum Theory of the Solid State* (Academic, New York, 1974).
[15]See also for example, S. K. Singwi, Phys. Rev. 176, 589 (1968).
[16]J. Rath and A. J. Freeman, Phys. Rev. B 11, 2109 (1975).
[17]N. E. Brener and J. L. Fry, Phys. Rev. B 19, 1720 (1979).
[18]L. Hedin, Phys. Rev. 139, A796 (1965).
[19]J. Callaway and J. L. Fry, in *Computational Methods in Band Theory*, edited by P. M. Marcus, J. F. Janak, and A. R. Williams (Plenum, New York, 1971), p. 512.
[20]D. M. Drost and J. L. Fry, Phys. Rev. B 5, 684 (1972).
[21]N. E. Brener and J. L. Fry, Phys. Rev. B 6, 4016 (1972).
[22]A. J. H. Wachters, J. Chem. Phys. 52, 1033 (1970).
[23]Thomas Wright, Commun. ACM 17, 152 (1974).
[24]L. F. Mattheiss, Phys. Rev. 139, A1893 (1965).
[25]N. E. Brener and J. L. Fry, Bull. Am. Phys. Soc. 23, 101 (1978).
[26]W. Koehler, R. M. Moon, A. L. Trego, and A. R. Mac Kintosh, Phys. Rev. 151, 405 (1966).
[27]C. S. Wang and J. Callaway, Comput. Phys. Commun. 14, 327 (1978).